



## Scalable Uplink Combining in Cell-Free Massive MIMO under Practical Fading and Centralized Processing

Mohammed H. Abuzgaia<sup>1\*</sup>, Mohamed A. Elalem<sup>2</sup>

<sup>1</sup>Electrical And Computer Engineering Department, Communications Field , Elmergib University, Faculty of Engineering , Al-Khmos, Libya, [m.abuzgaia@gmail.com](mailto:m.abuzgaia@gmail.com)

<sup>2</sup>Electrical And Computer Engineering Department, Communications Field , Elmergib University, Faculty of Engineering, Al-Khmos, Libya, [maelalem@elmergib.edu.ly](mailto:maelalem@elmergib.edu.ly)

\*Corresponding author: [m.abuzgaia@gmail.com](mailto:m.abuzgaia@gmail.com)

Received: 09 Feb 2026

Accepted: 23 Feb 2026

Published: 01 March 2026

### Abstract

In this paper, we conducted a performance study of uplink combining algorithms for Cell-Free Massive MIMO, a future wireless technology aimed at removing cell boundaries to reduce inter-cell interference. In contrast to traditional Massive MIMO, Cell-Free deployments adopt multiple distributed access points (APs) that cooperate to serve users, thereby increasing spectral efficiency (SE) and service fairness. We analyze centralized combining schemes such as MMSE, MR, ZF, and RZF under both Rayleigh and Rician fading environments, considering fronthaul and complexity constraints. System-level simulations evaluate SE behavior for different numbers of APs and antennas. Comparisons indicate that the MMSE and RZF have achieved SE but with higher complexity. The 90%-likely SE is used as a measure of fairness and reliability.

**Keywords:** Massive MIMO, MMSE, P-MMSE, ZF, RZF, TPE-MR, TPE-MMSE, SE, CDFs.

### 1. Introduction

Fifth Generation (5G) mobile communication systems have emerged in response to the exponential increase in connected devices and the growing demand for ultra-reliable, high-speed data services. To meet these demands, 5G aims to deliver multi-gigabit-per-second data rates, ultra-low latency, high reliability, enhanced network capacity, and consistent user experiences across diverse applications, including the Internet of Things (IoT) and smart technologies. A key enabler of these capabilities is Massive Multiple-Input Multiple-Output (Massive MIMO), wherein base stations equipped with large antenna arrays simultaneously serve multiple users over the same time-frequency resources. This architecture provides high spectral efficiency, improved reliability, and energy-efficient operation through relatively simple linear signal processing techniques [1], [2]. Massive MIMO arrays can be deployed in either collocated or distributed configurations. While collocated deployments minimize backhaul requirements, distributed Massive MIMO, where antennas are geographically



dispersed, offers superior macro-diversity and higher coverage probability, especially under shadow fading, albeit with increased fronthaul demands [3].

Massive MIMO is widely recognized as a scalable solution for the physical layer of 5G systems [1], [4], [5]. Unlike conventional multi-user MIMO, which requires full channel state information (CSI) and complex dirty paper coding at both transmitter and receiver ends [6], [7], [8] Massive MIMO relies on CSI available only at the base station and employs simple linear precoding, making it highly scalable. Traditional multi-cell Massive MIMO involves co-located antennas serving users within defined cells [2]. In contrast, Cell-Free Massive MIMO redefines this paradigm by deploying a large number of distributed single-antenna Access Points (APs), all connected to a Central Processing Unit (CPU), an edge cloud, via fronthaul links [9]. These APs cooperatively serve all users across the network area through coherent joint transmission and reception [10], [11]. In this architecture, users are not associated with specific APs; instead, all APs serve all users simultaneously using the same time-frequency resources. This approach eliminates inter-cell interference, maximizes macro-diversity, and provides a uniform quality of service across the network.

## 2. Channel Characteristics and Estimation

In Cell-Free Massive MIMO systems, the wireless channel is subject to multipath propagation, small-scale fading, and Doppler effects, which significantly impact signal quality and spectral efficiency. This section provides a comprehensive examination of wireless channel modeling and estimation techniques, focusing on their relevance to large-scale distributed antenna systems.

### A. Channel Modeling under Fading

Wireless channels are modeled using statistical fading distributions to capture environmental effects:

- **Rayleigh fading** is used for Non-Line-of-Sight (NLOS) scenarios, where the received signal comprises scattered multipath components [12].

$$P(r) = \left(\frac{r}{\sigma^2}\right) \exp\left(-\frac{r^2}{2\sigma^2}\right) \quad (1)$$

where  $P(r)$  is the probability of a particular amplitude,  $r$  is the signal amplitude,  $\sigma$  is the scale parameter of the distribution.

- **Rician fading** incorporates both a deterministic Line-of-Sight (LOS) component and scattered paths, representing more structured propagation environments [13].

$$\mathbf{P}(r) = \left(\frac{r}{\sigma^2}\right) \exp\left(-\frac{(r^2 + A^2)}{2\sigma^2}\right) \mathbf{I}_0\left(\frac{Ar}{\sigma^2}\right) \quad (2)$$

where  $\mathbf{P}(r)$  is the probability of a particular amplitude,  $r$  is the signal amplitude,  $\sigma$  is the scale parameter of the distribution,  $A$  is the amplitude of the LOS component and  $\mathbf{I}_0$  is the modified Bessel function of the first kind of order 0.

These models in addition to Nakagami-m [14] they are fundamental in simulating realistic scenarios and evaluating the robustness of combining techniques in the presence of channel variability.

### B. MMSE Channel Estimation

The Minimum Mean Square Error (MMSE) estimator is widely adopted in massive MIMO systems due to its superior accuracy under Gaussian noise assumptions. It minimizes the expected square error between the true and estimated channels using prior channel statistics. The MMSE estimate is given by:

$$\hat{\mathbf{h}}_{MMSE} = \mathbf{R}_{hh} \mathbf{R}_{hy}^{-1} \mathbf{y} \quad (3)$$

where  $\mathbf{R}_{hh}$  is the autocorrelation matrix of the channel, and  $\mathbf{R}_{hy}$  is the cross-correlation matrix between the channel and the received signal [15]. Compared to simpler methods like Least Squares (LS) and Maximum Likelihood (ML), MMSE achieves the lowest estimation error but requires knowledge of second-order channel statistics and involves matrix inversion, making it computationally intensive [16].

### C. Uplink Training and Pilot Contamination

Pilot-based uplink training is essential for acquiring accurate CSI in TDD-based Cell-Free Massive MIMO systems. However, pilot contamination caused by the reuse of pilot sequences across users can significantly degrade estimation accuracy. To mitigate pilot contamination:

- Orthogonal and reuse-aware pilot allocation strategies are implemented.
- Power control mechanisms dynamically adjust pilot transmission power.
- Advanced techniques such as interference-aware training and user clustering are employed to improve channel estimation robustness under mobility and dense deployment scenarios.

Time-variant fading, Doppler spread, and frequency selectivity further complicate estimation, especially in high-mobility or wideband systems, where adaptive and robust channel tracking are necessary.

### 3. Cell-Free Massive MIMO: Architectures And Challenges.

Massive MIMO has emerged as a foundational technology for 5G and beyond, enabling substantial gains in spectral and energy efficiency through spatial multiplexing, beamforming, and interference suppression. This section presents a comparative analysis between conventional massive MIMO systems and the more recent Cell-Free Massive MIMO paradigm, highlighting architectural distinctions, benefits, and implementation challenges.

#### A. Conventional Massive MIMO

Massive MIMO systems rely on co-located antenna arrays at centralized base stations to serve multiple users simultaneously over the same time-frequency resources. Key advantages include:

- High spectral efficiency through spatial multiplexing.
- Improved energy efficiency via beamforming.
- Enhanced interference suppression by exploiting large antenna arrays.

However, traditional massive MIMO is constrained by:

- Inter-cell interference, especially at cell edges.
- Pilot contamination in multicell scenarios.
- Limited scalability due to centralized processing and hardware complexity [1], [17].

#### B. Cell-Free Massive MIMO Architecture

Cell-Free Massive MIMO removes cell boundaries by deploying a large number of geographically distributed APs, all jointly serving users through coherent processing. The APs are connected to one or more CPUs, forming a user-centric, network-wide MIMO system [18], [19].

##### ❖ Advantages of Cell-Free Massive MIMO:

- **Macro-diversity:** Increased resilience to fading and shadowing due to spatial diversity.
- **Uniform Quality-of-Service (QoS):** Eliminates coverage holes and cell-edge degradation.
- **Scalability:** User-centric clustering and distributed processing allow flexible expansion [20].

The uplink and downlink signal processing tasks can be allocated between the APs and the CPUs in various architectures, as illustrated in Figure.1.

- **Centralized operation:** All baseband signal processing operations—including channel estimation, receive combining, and data detection—are executed at the CPU. While this

approach enables globally optimal performance through joint processing, it imposes significant fronthaul capacity and latency requirements due to the need to transfer raw or partially processed signals from all APs.

- **Distributed operation:** Signal processing tasks such as channel estimation, combining, and precoding are carried out locally at each AP. This architecture reduces fronthaul load and computational burden at the CPU, making it more scalable for large-scale deployments. However, performance may be suboptimal compared to centralized schemes due to the lack of global channel state information.

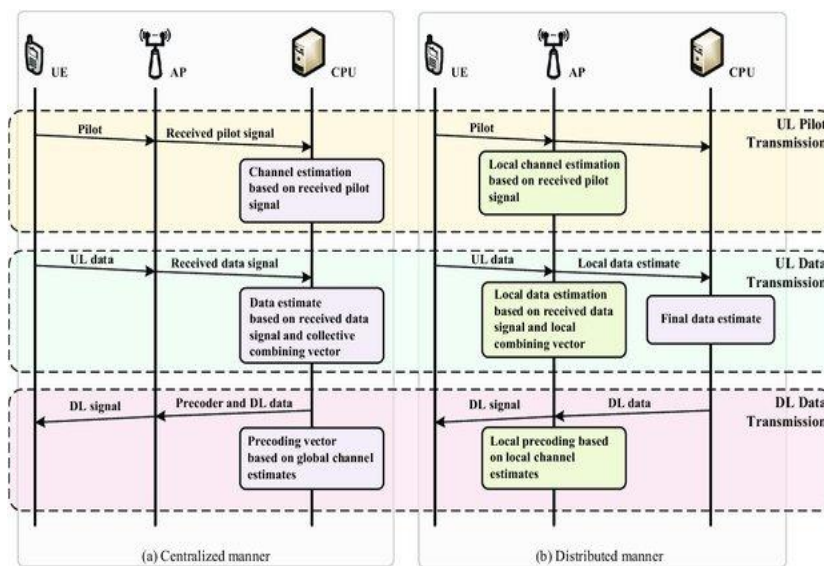


**Figure.1:** Centralized vs. Distributed Operation in Cell-Free Massive MIMO [21].

### C. Scalability in Cell-Free Massive MIMO Networks

Ensuring scalability is critical for next-generation wireless systems with wide geographic coverage. A scalable architecture enables the seamless addition of APs and User Equipments (UEs) without modifying the existing infrastructure.

Unlike cellular systems, scalability in Cell-Free Massive MIMO is more complex due to the cooperative service of all UEs by all APs. Each AP may directly or indirectly serve UEs, subject to constraints such as limited computational resources and fronthaul capacity. As the network grows in users or APs, these resources must remain manageable.

To assess scalability, consider an asymptotic regime where the number of users  $K \rightarrow \infty$ . Each AP must still be able to perform:

- Channel estimation,
- Uplink/downlink data processing,

- Fronthaul signaling for CSI and data,
- Power control and resource allocation.

**Definition 1 (Scalability):** A Cell-Free Massive MIMO network is scalable if each AP can carry out all required operations with finite computational and fronthaul resources as  $K \rightarrow \infty$  [22].

This definition emphasizes algorithmic tractability in large-scale deployments. It permits centralized processing as long as resource demands do not scale with  $K$  [23].

To address scalability and interference, the Dynamic Cooperation Clustering (DCC) framework is adopted:

**Definition 2 (DCC):** A user-centric scheme where each AP serves a subset of UEs based on channel conditions. This approach enables a unified analysis of various communication scenarios, ranging from interference channels to network MIMO systems. To implement this framework, a set of diagonal matrices  $\mathcal{D}_{il} \in \mathbb{C}^{N \times N}$ , for  $i = 1, \dots, K$  and  $l = 1, \dots, L$  is defined to determine which AP antennas are permitted to transmit to or receive signals from specific UEs.

More precisely, the diagonal element of  $\mathcal{D}_{il}$  is set to 1 if the antenna of AP  $l$  is authorized to transmit to and decode signals from UE  $i$ ; otherwise, it is set to 0. This can be expressed as

$$\mathcal{D}_{il} = \begin{cases} \mathbf{I}_N & \text{if } l \in \mathcal{M}_i \\ \mathbf{0}_N & \text{if } l \notin \mathcal{M}_i \end{cases} \quad (4)$$

where  $\mathbf{I}_N$  and  $\mathbf{0}_N$  are identity matrix and zero matrix of dimension  $N$  respectively,  $\mathcal{M}_i$  represents the set of APs that are selected to serve UE  $i$ . This mechanism allows for efficient management of transmission resources and minimizes interference by dynamically adjusting the cooperation clusters based on the channel state information [22].

#### 4. Spectral Efficiency and Scalability of Cell-Free Massive MIMO.

This section formulates the uplink spectral efficiency analysis in Cell-Free Massive MIMO systems under both centralized and distributed operation frameworks. The analysis is built upon a realistic system model with pilot-based channel estimation, scalable combining schemes, and fronthaul-aware architectural constraints. Key contributions include mathematical derivation of achievable SE expressions and comparative evaluation across combining techniques under Rayleigh and Rician fading environments.

## A. System Model and Pilot-Based Channel Estimation

The Cell-Free system comprises  $M$  access points, each equipped with  $N$  antennas, jointly serving  $K$  users using Time-Division Duplexing (TDD). The communication frame is divided into uplink training, data transmission, and downlink phases. During the uplink training phase, users transmit orthogonal pilot sequences of length  $\tau_p$  to enable MMSE-based channel estimation [24].

The estimated channel is then used in the uplink to coherently combine the received signals, either at a centralized processing unit or locally at each AP. Pilot contamination due to reuse of non-orthogonal pilots in densely deployed networks is considered in the derivation of achievable SE.

## B. Achievable Uplink Spectral Efficiency

The uplink SE for user  $k$  is lower-bounded using the use-and-then-forget (UatF) bound [18]:

$$SE_k = \left(1 - \frac{\tau_p}{\tau_c}\right) \log_2(1 + \text{SINR}_k) \quad (5)$$

where  $\tau_c$  is the coherence block length, and  $\text{SINR}_k$  is the effective post-combining signal-to-interference-plus-noise ratio for user  $k$ , which depends on the combining scheme and system architecture.

## C. Centralized Combining Techniques

Centralized operation assumes that all APs send received signals to the CPU, which performs joint channel estimation, receive combining, and detection. The following combining schemes are analyzed:

- **MMSE and Partial MMSE (P-MMSE):** Offers optimal performance but with high computational and fronthaul overhead.
- **Zero-Forcing (ZF) and Regularized ZF (RZF):** Provides better interference suppression than MR, with RZF balancing between MMSE and ZF.
- **Truncated Polynomial Expansion (TPE-MR and TPE-MMSE):** Polynomial approximations to reduce complexity while retaining high performance [25].

## 5. Uplink Combining in Cell-Free MIMO: Simulation under Fading and Modes.

This section outlines the simulation environment employed to evaluate the performance of uplink spectral efficiency in Cell-Free Massive MIMO systems. The analysis compares

centralized and scalable implementations of multiple linear combining techniques under both Rayleigh and Rician fading conditions. The goal is to provide a comprehensive understanding of how architectural choices, fading environments, and combining strategies affect the distribution and fairness of SE among users.

### A. Network Configurations:

Two distinct scenarios are considered:

- **Scenario (a):** 400 access points, each equipped with a single antenna ( $N = 1$ ).
  - **Scenario (b):** 100 access points, each equipped with four antennas ( $N = 4$ ).
- Each scenario is evaluated under both Rayleigh and Rician fading conditions.

### B. Simulation Parameters:

Table I lists the simulation parameters used throughout the evaluation.

**Table I:** Simulation Parameters

Symbol	Description	Value
$\alpha$	Path loss exponent	3.76
$d$	Antenna spacing in wavelengths	$0.5 \lambda$
$ASD_{deg}$	Angular standard deviation around nominal angle	20 degrees
B	Communication bandwidth	20 MHz
constantTerm	Average channel gain at 1 m reference distance	-35.3dB
K	Number of UEs in the network	100
nbrOfRealizations	Number of small-scale fading realizations per setup	1000
nbrOfSetups	Number of Monte Carlo setups	25
noiseFigure	Receiver noise Figure	7dB
p	Uplinks transmit power per UE	100 mW
$\sigma_{sf}$	Shadow fading standard deviation	10 dB
squareLength	Side length of the square service area with wrap-around	2000
$\tau_c$	Coherence block length (channel uses)	200
$\tau_p$	Pilot sequence length	10
threshold	Serving threshold for non-master Aps	-40 dB
L	Number of APs per setup	400 and 100
N	Number of antennas per AP	1 and 4

### C. Simulation Methodology:

All access points are connected to a CPU in the centralized architecture, which performs channel estimation and signal combining. In scalable implementations, local processing at APs reduces the fronthaul burden at the cost of performance degradation. Uplink SE is calculated for each user in every realization, and results are averaged across Monte Carlo setups. The fairness metric used is the 90%-likely SE, representing the spectral efficiency value below

which 10% of the users fall. This metric effectively captures the system's ability to provide uniformly good service to most users.

#### D. Performance Results:

The uplink SE distributions for each combining scheme are visualized through cumulative distribution functions (CDFs). Performance is assessed under both Rayleigh and Rician fading for each network configuration.

- **MMSE vs. P-MMSE (Scalable MMSE):**

- Rayleigh fading (Figure.2): MMSE outperforms P-MMSE with 90%-likely SEs of 2.97 in (a) and 1.66 bit/s/Hz in (b) , compared to 2.35 and 1.16 bit/s/Hz.

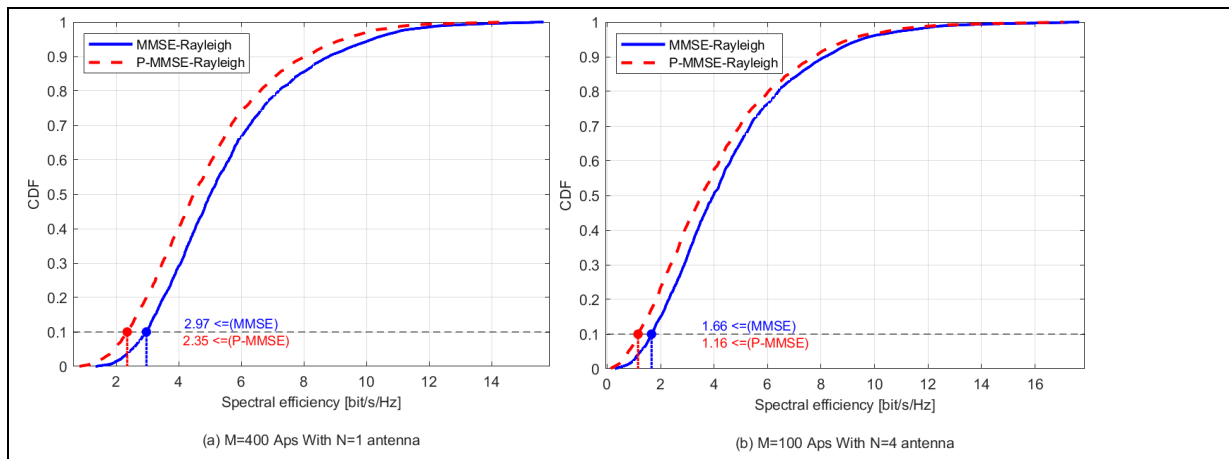


**Figure.2:** UL SE per UE with MMSE and P-MMSE (scalable MMSE) in Rayleigh fading case.

- Rician fading (Figure.3): MMSE achieves 11.79 and 8.37 bit/s/Hz, significantly higher than P-MMSE (1.06 and 1.61 bit/s/Hz).

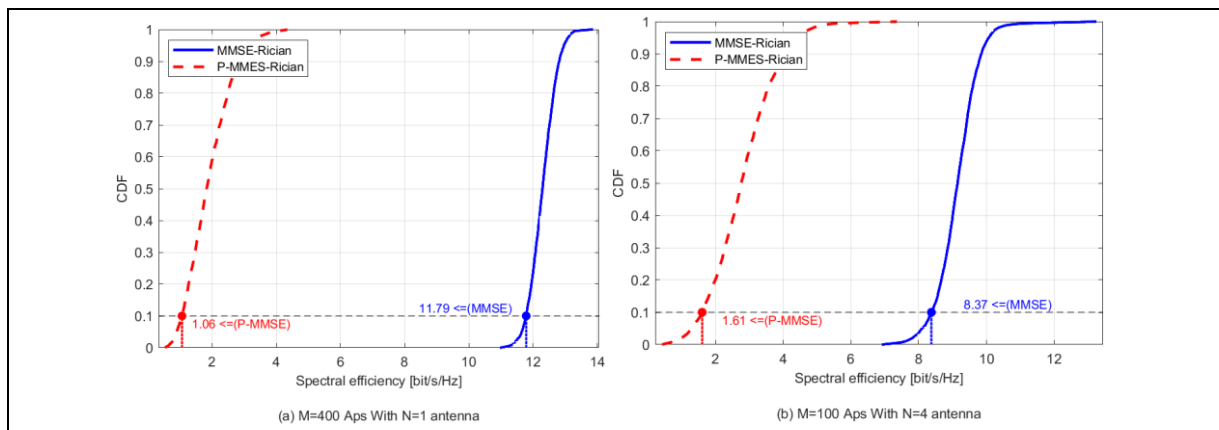




**Figure.3:** UL SE per UE with MMSE and P-MMSE (scalable MMSE) in Rician fading case.



• **ZF vs. Scalable ZF:**

- Rayleigh fading (Figure.4): ZF yields 2.78 and 1.52 bit/s/Hz; Scalable ZF drops to 1.52 and 0.58 bit/s/Hz.

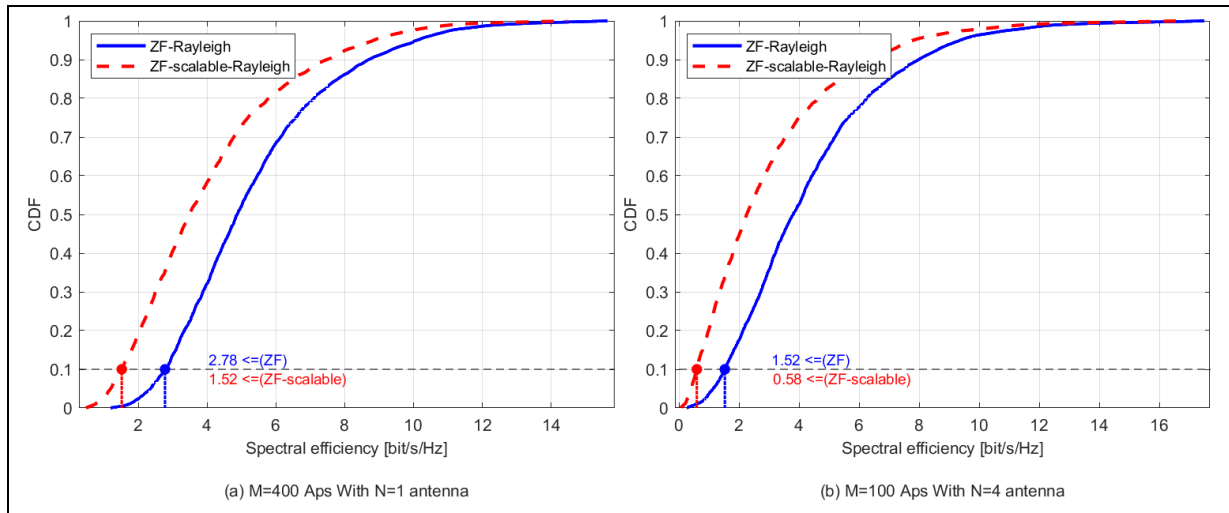


**Figure.4:** UL SE per UE with ZF and Scalable ZF in Rayleigh Fading Case.

- Rician fading (Figure.5): ZF reaches 11.55 and 8.15 bit/s/Hz, while Scalable ZF only attains 1.12 and 2.21 bit/s/Hz.

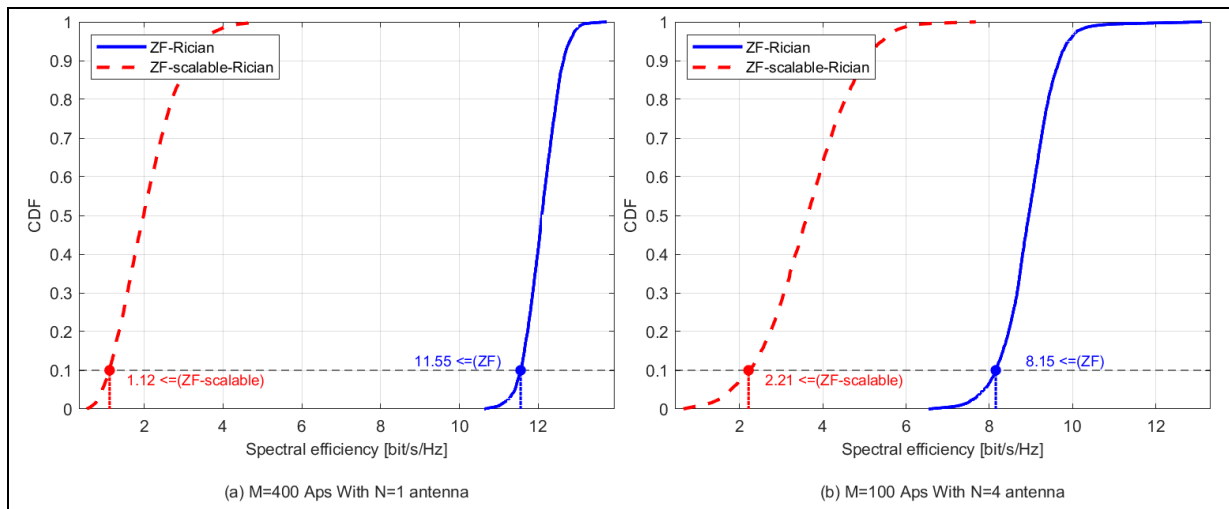


**Figure.5:** UL SE per UE with ZF and Scalable ZF in Rician Fading Case.

• **RZF vs. Scalable RZF:**

- Rayleigh fading (Figure.6): Centralized RZF yields 2.8 and 1.53 bit/s/Hz; Scalable RZF provides 1.55 and 0.58 bit/s/Hz.

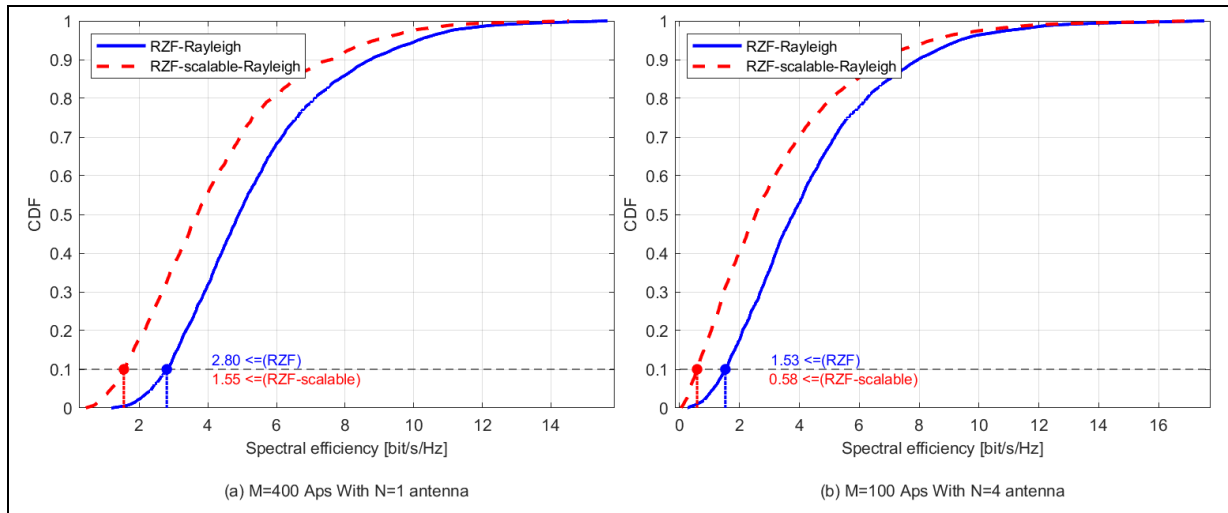


**Figure.6:** UL SE per UE with RZF and Scalable RZF in Rayleigh Fading Case.

- Rician fading (Figure.7): Centralized RZF reaches 11.55 and 8.16 bit/s/Hz, outperforming scalable versions (1.12 and 2.14 bit/s/Hz).

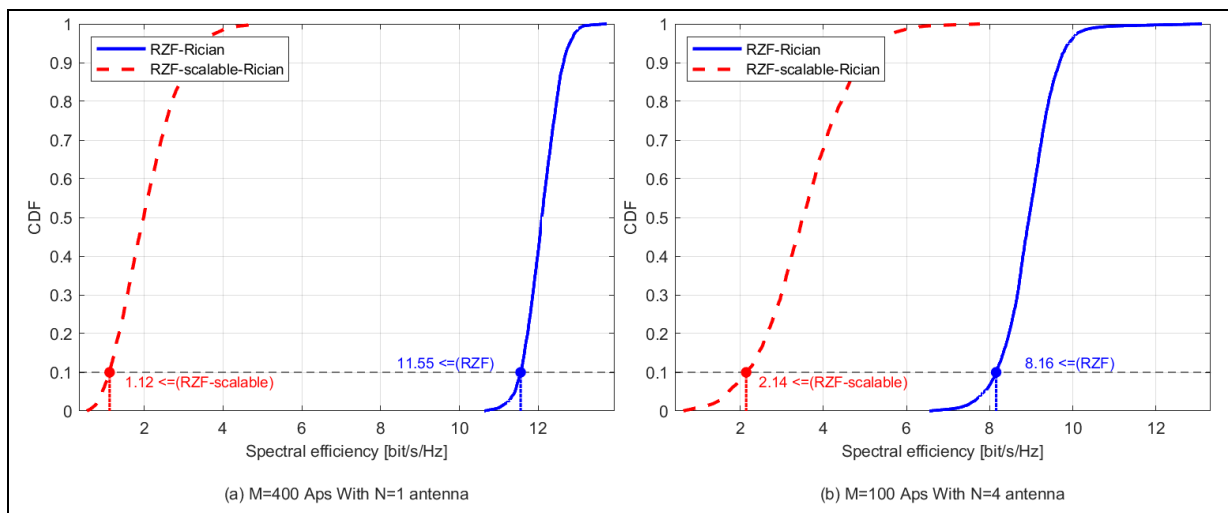


**Figure.7:** UL SE per UE with RZF and Scalable RZF in Rician Fading Case.

• TPE-MR and Scalable TPE-MR:

- Rayleigh fading (Figure.8): Both yield 0.00 bit/s/Hz across configurations due to poor interference mitigation.

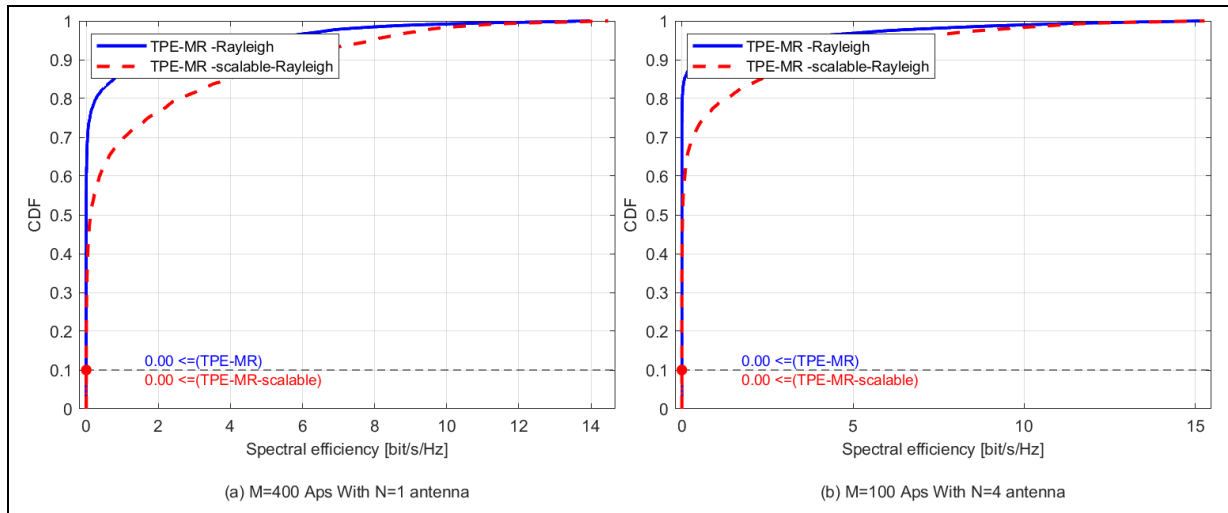


Figure.8: UL SE per UE with TPE-MR and Scalable TPE-MR in Rayleigh Fading Case.

- Rician fading (Figure.9): Scalable version achieves 0.3 and 0.17 bit/s/Hz; centralized version remains at 0.01 bit/s/Hz.

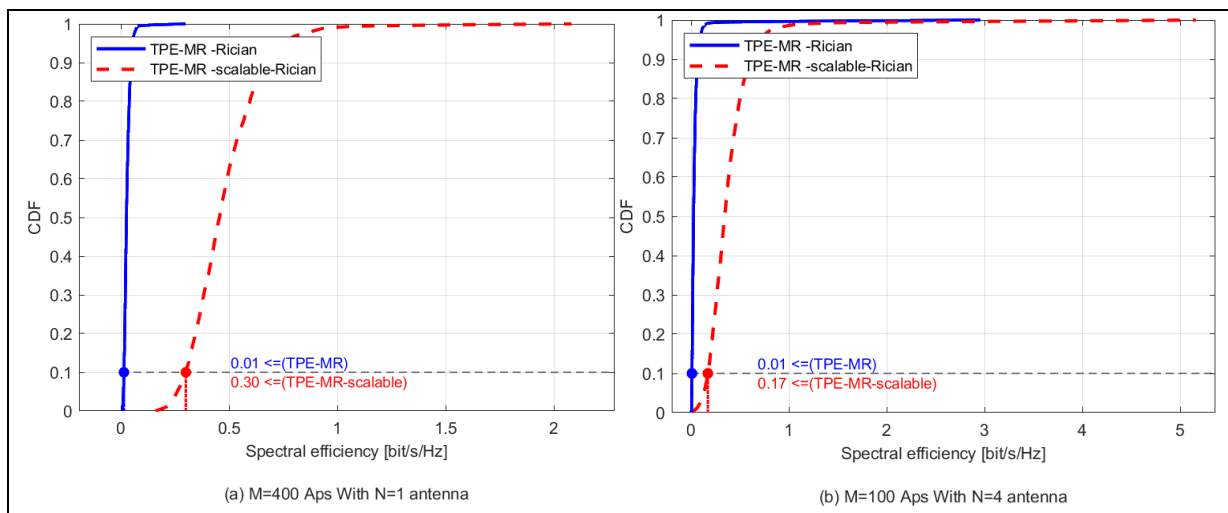
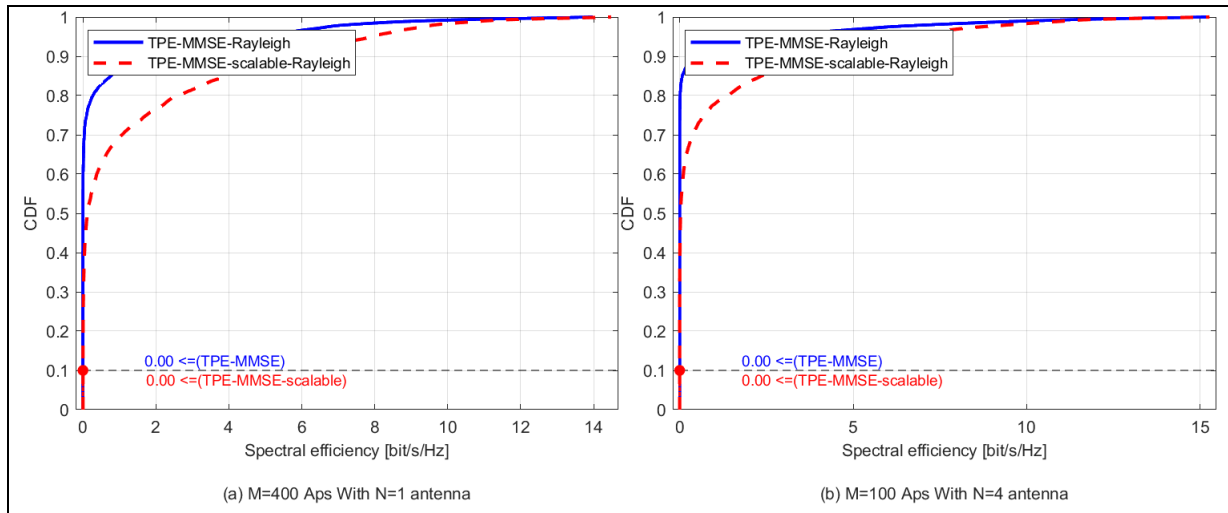


Figure.9: UL SE per UE with TPE-MR and Scalable TPE-MR in Rician Fading Case.

• TPE-MMSE and Scalable TPE-MMSE:

- Rayleigh fading (Figure.10): Both variants exhibit 0.00 bit/s/Hz, highlighting limitations of polynomial expansion.



**Figure.10:** UL SE per UE with TPE-MMSE and Scalable TPE-MMSE in Rayleigh Fading Case.

- Rician fading (Figure.11): Scalable variant yields 0.3 and 0.17 bit/s/Hz; centralized reaches only 0.01 bit/s/Hz.

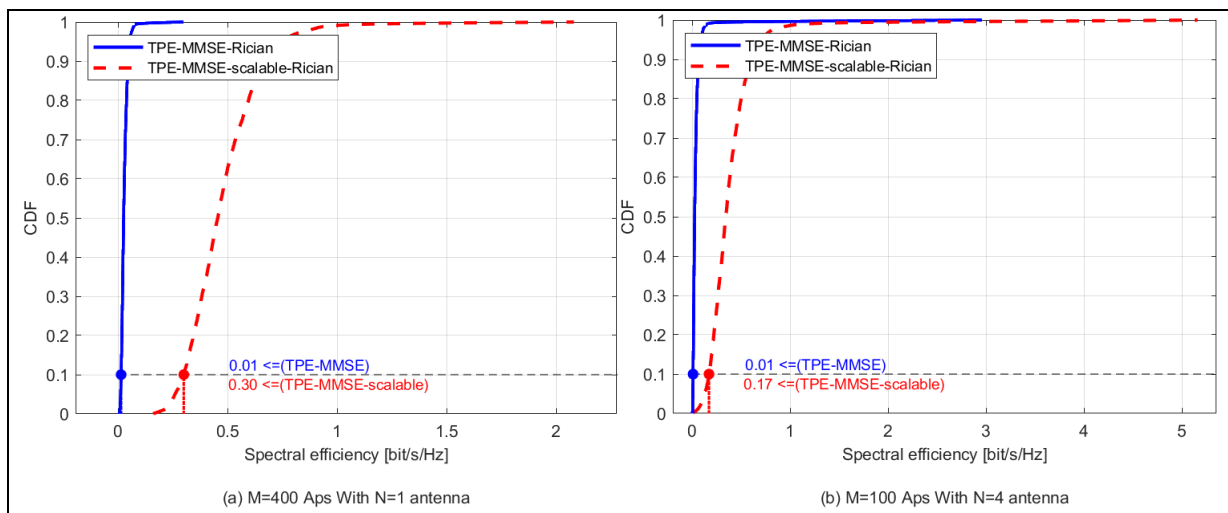


**Figure.11:** UL SE per UE with TPE-MMSE and Scalable TPE-MMSE in Rician Fading Case.



### E. Key observations from the simulations:

- MMSE provides the highest SE and fairness among all combining techniques.
- ZF and RZF are also effective under centralized operation, but degrade significantly in a scalable form.
- TPE-based methods fail to suppress interference efficiently, yielding poor SE under Rayleigh fading.
- The presence of a LOS component (Rician fading) significantly boosts performance, especially for centralized MMSE and ZF.
- Increasing the number of APs ( $M$ ) improves spatial diversity and fairness.
- Increasing the number of antennas per AP ( $N$ ) is beneficial for distributed setups by enhancing beamforming and reducing reliance on global CSI.

## 6. Conclusion

Centralized combining techniques consistently outperform their scalable counterparts, particularly in interference-limited Rayleigh environments. The presence of a Line-of-Sight component in Rician fading enhances performance across all uplink combining techniques, with MMSE and ZF benefiting the most due to their ability to effectively exploit the deterministic channel component. MMSE and P-MMSE consistently achieve the highest spectral efficiency under both Rayleigh and Rician fading conditions, with MMSE slightly outperforming P-MMSE as it leverages full channel state information. ZF and RZF also demonstrate strong performance, particularly in moderate-to-high SNR regimes and interference-limited scenarios. In contrast, MR and TPE-MR yield lower SE but remain attractive for their simplicity and scalability. TPE-MMSE offers a favorable complexity-performance trade-off by approximating MMSE behavior with reduced computational burden, however, its limited robustness in dense deployments and under fairness constraints—measured via 90%-likely SE—underscores the need for more advanced solutions. Increasing the number of access point ( $M$ ) enhances spatial diversity and mitigates inter-user interference, significantly improving fairness and performance, especially in centralized setups. On the other hand, increasing the number of antennas per AP ( $N$ ) strengthens local beamforming gains and is particularly advantageous in distributed architectures. Overall, the performance gap between low-complexity and optimal schemes highlights the potential of hybrid or higher-order methods as promising directions for future research.





## References

- [1] T. L. Marzetta, "Noncooperative Cellular Wireless with Unlimited Numbers of Base Station Antennas," *IEEE Trans. Wirel. Commun.*, vol. 9, no. 11, pp. 3590–3600, Nov. 2010, doi: 10.1109/TWC.2010.092810.091092.
- [2] H. Yang and T. L. Marzetta, "A macro cellular wireless network with uniformly high user throughputs," in *IEEE Vehicular Technology Conference*, IEEE, Sep. 2014, pp. 1–5. doi: 10.1109/VTCFall.2014.6965818.
- [3] S. Zhou, M. Zhao, X. Xu, J. Wang, and Y. Yao, "Distributed wireless communication system: A new architecture for future public wireless access," *IEEE Communications Magazine*, vol. 41, no. 3, pp. 108–113, 2003, doi: 10.1109/MCOM.2003.1186553.
- [4] F. Rusek, D. Persson, Buon Kiong Lau, E. G. Larsson, T. L. Marzetta, and F. Tufvesson, "Scaling Up MIMO: Opportunities and Challenges with Very Large Arrays," *IEEE Signal Process. Mag.*, vol. 30, no. 1, pp. 40–60, Jan. 2013, doi: 10.1109/MSP.2011.2178495.
- [5] F. Boccardi, R. Heath, A. Lozano, T. L. Marzetta, and P. Popovski, "Five disruptive technology directions for 5G," *IEEE Communications Magazine*, vol. 52, no. 2, pp. 74–80, Feb. 2014, doi: 10.1109/MCOM.2014.6736746.
- [6] G. Caire and S. Shamai, "On the achievable throughput of a multiantenna Gaussian broadcast channel," *IEEE Trans. Inf. Theory*, vol. 49, no. 7, pp. 1691–1706, Jul. 2003, doi: 10.1109/TIT.2003.813523.
- [7] P. Viswanath and D. N. C. Tse, "Sum capacity of the vector Gaussian broadcast channel and uplink-downlink duality," *IEEE Trans. Inf. Theory*, vol. 49, no. 8, pp. 1912–1921, Aug. 2003, doi: 10.1109/TIT.2003.814483.
- [8] S. Vishwanath, N. Jindal, and A. Goldsmith, "Duality, achievable rates, and sum-rate capacity of Gaussian MIMO broadcast channels," *IEEE Trans. Inf. Theory*, vol. 49, no. 10, pp. 2658–2668, Oct. 2003, doi: 10.1109/TIT.2003.817421.
- [9] A. Burr, M. Bashar, and D. Maryopi, "Ultra-dense Radio Access Networks for Smart Cities: Cloud-RAN, Fog-RAN and 'cell-free' Massive MIMO," Jul. 2023, [Online]. Available: <http://arxiv.org/abs/1811.11077>
- [10] E. Björnson and E. Jorswieck, "Optimal Resource Allocation in Coordinated Multi-Cell Systems," *Foundations and Trends® in Communications and Information Theory*, vol. 9, no. 2–3, pp. 113–381, 2013, doi: 10.1561/01000000069.
- [11] S. Venkatesan, A. Lozano, and R. Valenzuela, "Network MIMO: Overcoming intercell interference in indoor wireless systems," in *Conference Record - Asilomar Conference on Signals, Systems and Computers*, IEEE, Nov. 2007, pp. 83–87. doi: 10.1109/ACSSC.2007.4487170.
- [12] J. J. Andrea, *Radio Wave Propagation Fundamentals*, 2nd Edition. Norwood, MA, USA: Artech House, 2018.
- [13] D. Giancrisofaro, "Correlation model for shadow fading in mobile radiochannels," *Electron. Lett.*, vol. 32, no. 11, pp. 958–959, May 1996, doi: 10.1049/el:19960655.





- [14] Tsan-Ming Wu, "Generation of Nakagami-m Fading Channels," in *2006 IEEE 63rd Vehicular Technology Conference*, IEEE, 2006, pp. 2787–2792. doi: 10.1109/VETECS.2006.1683376.
- [15] Y. S. Cho, J. Kim, W. Y. Yang, and C. G. Kang, *MIMO-OFDM Wireless Communications with MATLAB®*. Wiley, 2010. doi: 10.1002/9780470825631.
- [16] D. Tse and P. Viswanath, *Fundamentals of Wireless Communication*. Cambridge University Press, 2005. doi: 10.1017/CBO9780511807213.
- [17] T. L. Marzetta, "Noncooperative Cellular Wireless with Unlimited Numbers of Base Station Antennas," *IEEE Trans. Wirel. Commun.*, vol. 9, no. 11, pp. 3590–3600, Nov. 2010, doi: 10.1109/TWC.2010.092810.091092.
- [18] H. Q. Ngo, A. Ashikhmin, H. Yang, E. G. Larsson, and T. L. Marzetta, "Cell-Free Massive MIMO Versus Small Cells," *IEEE Trans. Wirel. Commun.*, vol. 16, no. 3, pp. 1834–1850, 2017, doi: 10.1109/TWC.2017.2655515.
- [19] E. Nayebi, A. Ashikhmin, T. L. Marzetta, and H. Yang, "Cell-Free Massive MIMO systems," *Conf. Rec. Asilomar Conf. Signals Syst. Comput.*, vol. 2016-Febru, pp. 695–699, 2016, doi: 10.1109/ACSSC.2015.7421222.
- [20] S. Buzzi, C. D'andrea, A. Zappone, and C. D'elia, "User-Centric 5G Cellular Networks: Resource Allocation and Comparison with the Cell-Free Massive MIMO Approach," *IEEE Trans. Wirel. Commun.*, vol. 19, no. 2, pp. 1250–1264, 2020, doi: 10.1109/TWC.2019.2952117.
- [21] S. Chen, J. Zhang, J. Zhang, E. Björnson, and B. Ai, "A Survey on User-Centric Cell-Free Massive MIMO Systems," Oct. 2021, [Online]. Available: <http://arxiv.org/abs/2104.13667>
- [22] E. Björnson and L. Sanguinetti, "Scalable Cell-Free Massive MIMO Systems," *IEEE Transactions on Communications*, vol. 68, no. 7, pp. 4247–4261, Jul. 2020, doi: 10.1109/TCOMM.2020.2987311.
- [23] Ö. T. Demir, E. Björnson, and L. Sanguinetti, "Foundations of user-centric cell-free massive MIMO," *Foundations and Trends in Signal Processing*, vol. 14, no. 3–4, pp. 162–472, Jan. 2021, doi: 10.1561/2000000109.
- [24] Hien Quoc Ngo, E. G. Larsson, and T. L. Marzetta, "Energy and Spectral Efficiency of Very Large Multiuser MIMO Systems," *IEEE Transactions on Communications*, vol. 61, no. 4, pp. 1436–1449, Apr. 2013, doi: 10.1109/TCOMM.2013.020413.110848.
- [25] S. Wagner, R. Couillet, M. Debbah, and D. T. M. Slock, "Large System Analysis of Linear Precoding in Correlated MISO Broadcast Channels Under Limited Feedback," *IEEE Trans. Inf. Theory*, vol. 58, no. 7, pp. 4509–4537, Jul. 2012, doi: 10.1109/TIT.2012.2191700.

